

The Structure Change of Dynamically Fatigued Unfilled Natural Rubber Vulcanizates

Ping Zhang,^{1,2} Xinyan Shi,¹ Junge Li,¹ Guangshui Yu,¹ Shugao Zhao^{1,2}

¹The Key Laboratory of Rubber-Plastics, Qingdao University of Science and Technology, Ministry of Education, Qingdao 266042, People's Republic of China

²The Key Laboratory of Nature Rubber Processing, Ministry of Agriculture, Zhanjiang 524000, People's Republic of China

Received 23 November 2007; accepted 29 March 2009

DOI 10.1002/app.30558

Published online 4 November 2009 in Wiley InterScience (www.interscience.wiley.com).

ABSTRACT: The submicrostructure of dynamically fatigued unfilled natural rubber vulcanizates was investigated by using scanning electron microscope (SEM) and atomic force microscope (AFM). AFM photographs showed the sample surface roughness became worse after tensile fatigue and the largest surface undulation was as twice that of the unfatigued sample. SEM photographs showed that many micropores of 10^1 – 10^2 nm, a sort of defect, occurred on the cross section of samples after tensile fatigue. The surface roughness became weaker and the size of the micropore was reduced to a few to dozens of nanometers with

the addition of antiaging agent *N*-(1,3-dimethyl butyl butyl)-*N'*-phenyl-*p*-phenylene diamine (4020); furthermore, the mechanical properties and dynamic viscoelastic properties in the later period of fatigue changed much. E' decreased greatly and $\tan \delta$ increased obviously with the extension of fatigue. It indicated that 4020 was only effective in the early period of tensile fatigue. © 2009 Wiley Periodicals, Inc. *J Appl Polym Sci* 115: 3535–3541, 2010

Key words: natural rubber; dynamic viscoelasticity; tensile fatigue; hot air aging; microscopic defect

INTRODUCTION

Natural rubber (NR) remains a major general purpose rubber due to its excellent cost/property ratio. NR plays an especially important role in products, such as tires, where its dynamic properties are required. Nowadays increasing attention is being paid to the wearing property of the material or articles, so it is of theoretical and practical significance that the changes of structure and dynamic viscoelastic properties of rubber materials or articles used under dynamic conditions would be explored and evaluated by using test methods that are close to the real working environment.

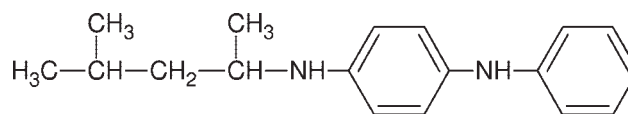
The submicrostructure of dynamically fatigued unfilled NR vulcanizates was investigated by using scanning electron microscope (SEM) and atomic force microscope (AFM). The antiaging function of *N*-(1,3-dimethyl butyl butyl)-*N'*-phenyl-*p*-phenylene diamine (4020) in unfilled NR vulcanizates was examined by using dynamic mechanical analysis (DMA), Fourier transform infrared attenuated total reflectance (FTIR-ATR), nuclear magnetic resonance, AFM, and SEM. It is hoped that exploration of the change rule of structure and dynamic viscoelastic

properties of NR vulcanizates after hot air aging and tensile fatigue will be used to correctly evaluate the security and reliability of the rubber articles used under dynamic conditions.

MATERIALS AND METHODS

Raw materials and basic formulation

NR SVR3L was acquired from Dong Nai Rubber (Dong Nai, Vietnam); antiaging agent 4020, with a molecular formula of



was manufactured by Nantong Nanhua Rubber Antiaging Agent Factory (Nantong, China). Others were bought from the market.

The formulation was 100 phr NR, 1.0 phr accelerator *N*-tert-butyl-2-benzothiazole sulfenamide, 5.0 phr zinc oxide, 2.0 phr stearic acid, 3.0 phr sulphur, and 1.0 phr antiaging agent 4020.

Specimen preparation

The specimens were prepared on an open mill according to GB6038-1993. The optimum cure time

Correspondence to: S. Zhao (zhaosgd@hotmail.com).

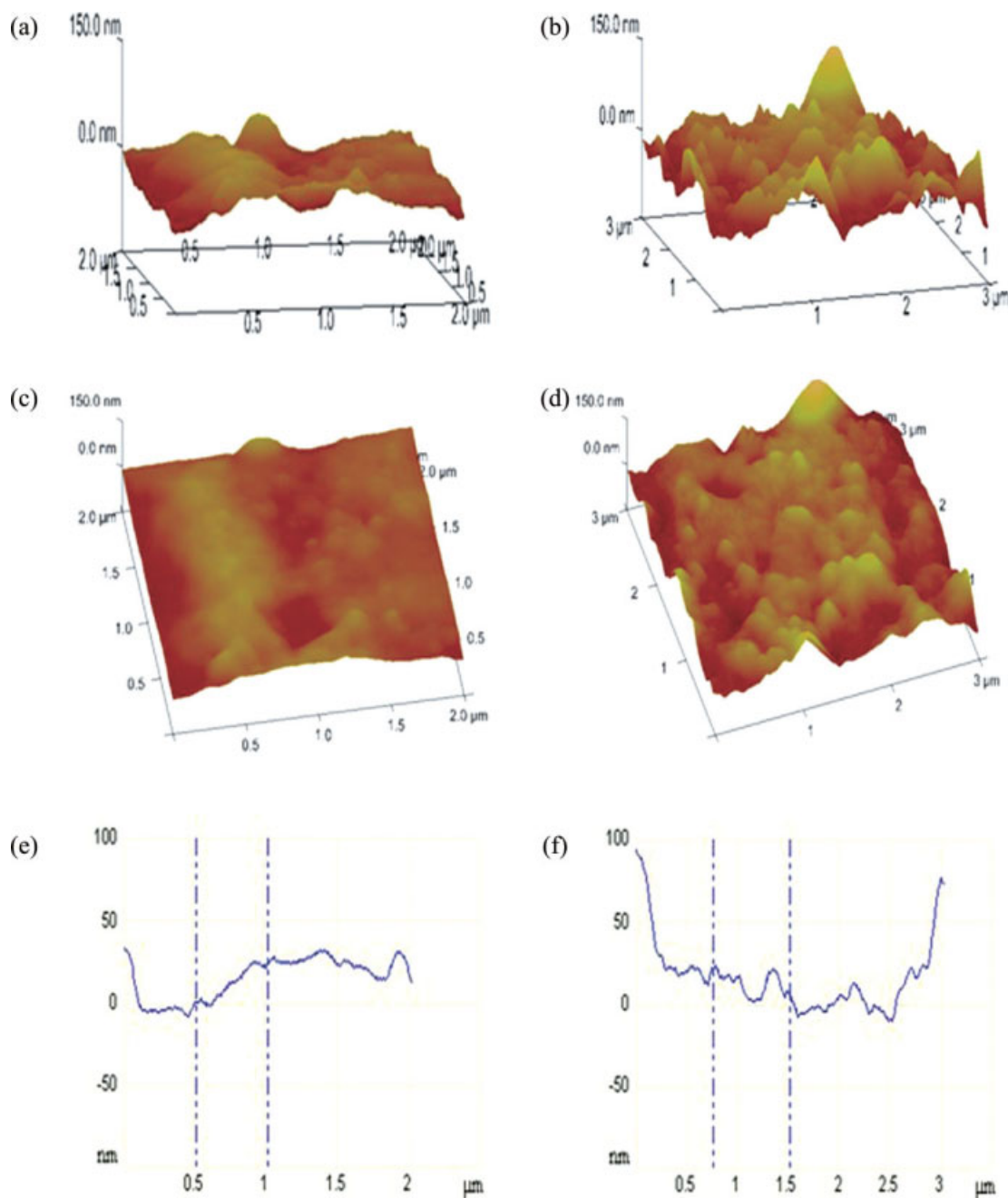


Figure 1 AFM photographs and sectional view along the line of unfilled NR vulcanizate before and after tensile fatigue (a: F0h; b: F6h; c: F0h; d: F6h; e: F0h; f: F6h). [Color figure can be viewed in the online issue, which is available at www.interscience.wiley.com.]

(t_{90}) was tested at 155°C with a GT-M2000-A cure meter manufactured by Gaotie Science and Technology (Taiwan, China). The compression moulding was carried out with a XIB press (manufactured by Qingdao Yadong Rubber and Plastics Machinery, Qingdao, China) at a pressure of 10 MPa.

Hot-air aging was carried out at 100°C for 24, 48, and 72 h with a 401A aging oven (manufactured by Shanghai Experiment Instruments Factory, Shanghai,

China) according to ISO 188:1998. Hot-air aged specimens were stored at room temperature for 2–3 h for further analysis.

Dynamic tensile fatigue was tested with a tensile fatigue tester (manufactured by Jiangdu Test Machinery Factory, Jiangdu, China) according to GB/1688–1986 with elongation of 100% and a tensile frequency of 500 min^{-1} . The specimens after tensile fatigue were stored at room temperature before further analysis.

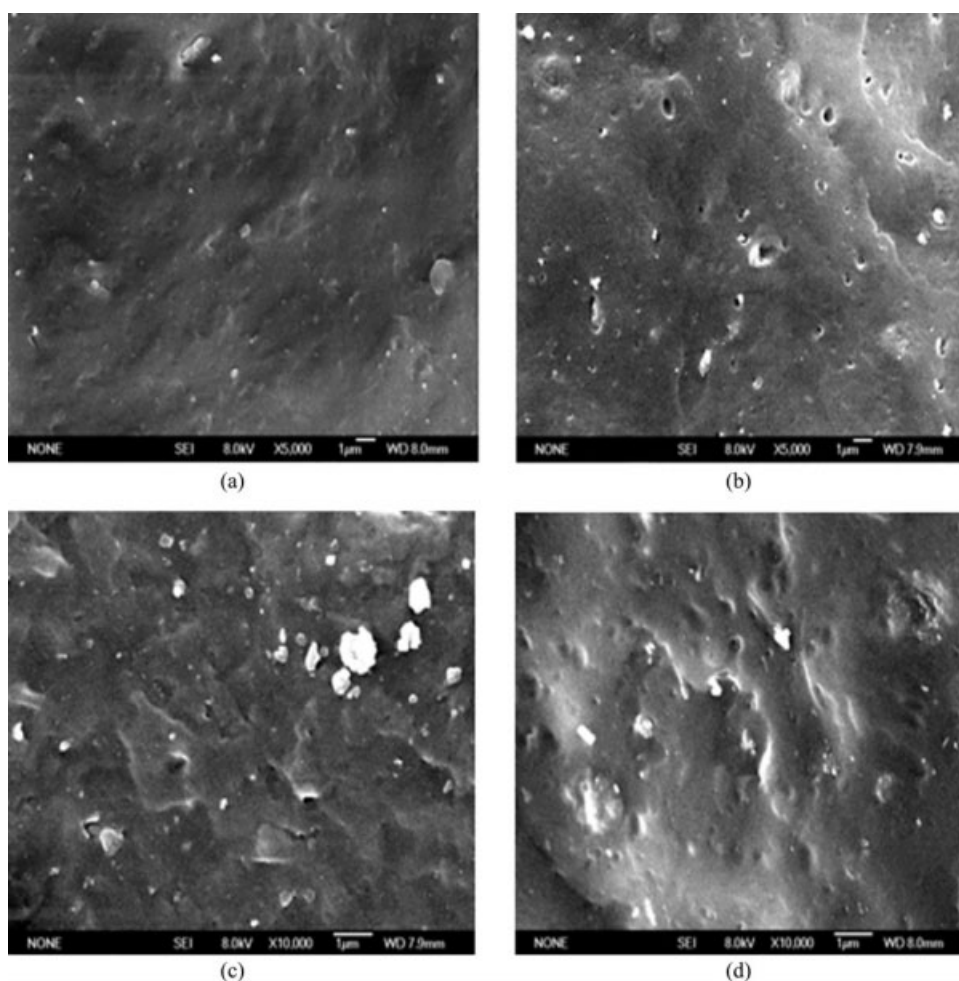


Figure 2 SEM photographs of unfilled NR vulcanizates before and after tensile fatigue. (a: F0h \times 5000; b: F6h \times 5000; c: F0h \times 10,000; d: F6h \times 10,000).

Tests and analysis

Tensile testing was carried out with a GT-AI-7000M universal material tester (manufactured by Taiwan Gaotie, Taiwan, China) at a tensile speed of 500 mm/min according to ISO 37:1994.

Crosslink density was measured with a MR-CDS 3500 crosslink density spectrometer (manufactured by IIC Innovative Imaging Corp., Blieskastel, Germany) with a magnetic field strength of 0.35 Tesla and a resonance frequency of 15 MHz at 60°C.

A column-shaped specimen 5 mm in diameter and 8 mm long was put into the bottom of a glass tube. The tube with the specimen was allowed to settle for 5 min until the magnetic field and temperature was stable, and then the test was started with the fixed parameters. The crosslink density of the vulcanizates was measured after the analysis of the data, as follows:

$$M(t) = A_0 + A_1 \exp(-t/T_2 - (qM_2 t^2)/2) + A_2 \exp(-t/T_2)$$

where $M(t)$ is the transversal magnetization dipolar moment (s^{-2}), t is decay time (ms), qM_2 is the

residual dipolar moment ($\sim 10^{-4} s^{-2}$), T_2 is the spin-spin relaxation time (ms), A_1 , A_2 are the amplitude factors, and A_0 is the fitting factor (no physical meaning).

Dynamic mechanical properties were tested with a NETZSCH 242 dynamic mechanical analyzer (Netzsch Instruments, Selb, Germany) with a frequency of 10 Hz, temperatures ranging from -80 to $+80^\circ\text{C}$, a heating rate of $3^\circ\text{C}/\text{min}$, and the mode of double cantilever deformation. Curves of $\tan \delta$ and E' as a function of temperature were examined.

FTIR spectra were produced with a Vertex70 spectrometer manufactured by Bruker (Ettlingen, Germany), and the attenuated total reflection mode was used to get the spectra.

SEM photographs were obtained on the surface of samples fractured in liquid nitrogen and coated with gold powder with a JSM-6700 SEM manufactured by Japan Electron Optics Laboratory (Tokyo, Japan).

AFM photographs were performed by tapping mode with Picoforce ATF manufactured by Veeco Instruments (New York, NY).

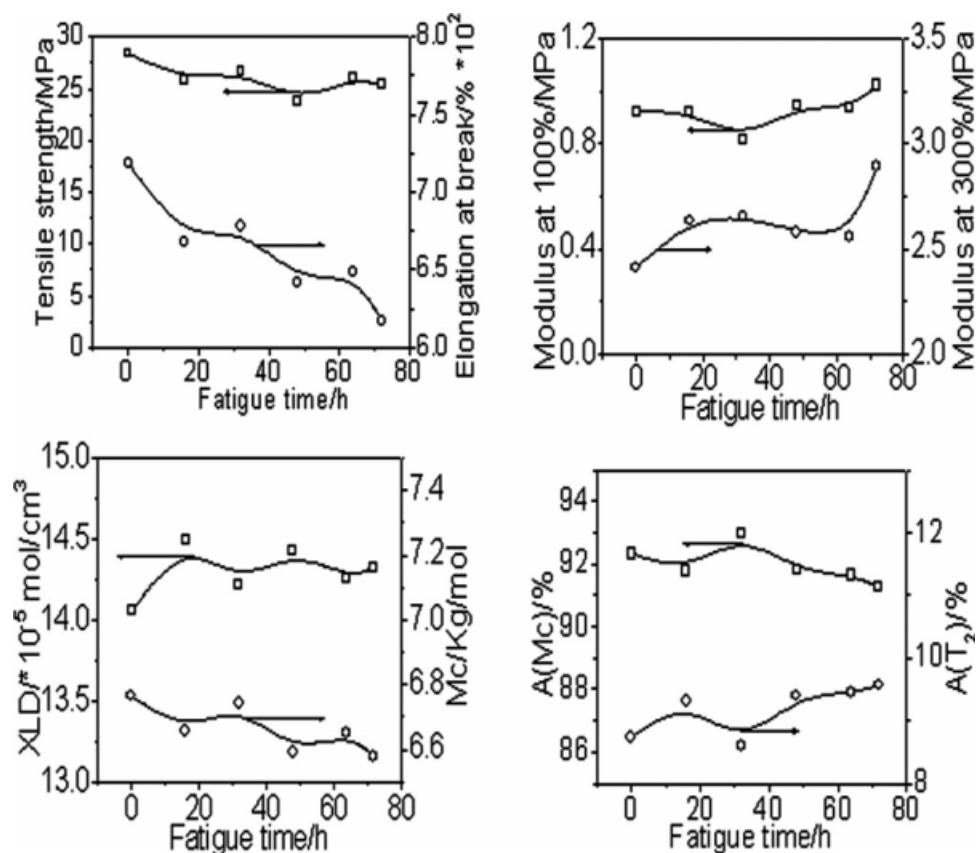


Figure 3 Mechanical properties and XLD of NR/4020 versus fatigue time.

RESULTS AND DISCUSSION

AFM and SEM analysis of dynamically fatigued unfilled natural rubber vulcanizates

In the former research work,¹ it has been known that the dynamic modulus E' decreased dramatically and the loss factor $\tan \delta$ increased greatly in the dynamically fatigued unfilled NR vulcanizates. To figure out the reasons, morphology of fatigued samples was examined by AFM and SEM as shown in Figures 1 and 2.

It can be seen in Figure 1(a,c) that the surface was not rough and relatively flat before tensile fatigue. Furthermore, the largest undulation was no more than 50 nm in Figure 1(e). However, the surface became rougher after 6 h of tensile fatigue as shown in Figure 1(b,d) and the largest undulation was nearly 100 nm in Figure 1(f).

As can be seen in Figure 2, there appeared some micropores of 10^1 – 10^2 nm on the cross section of samples after 6 h of tensile fatigue and those micropores looked shallow in the 10,000 magnification photographs. This may be attributed to the expansion of original defect and break of some bunches of molecular chains during tensile fatigue.

Through the above morphology analysis, it is concluded that tensile fatigue not only deteriorated the surface roughness, which could increase the probability of defect arising or stress concentration, but

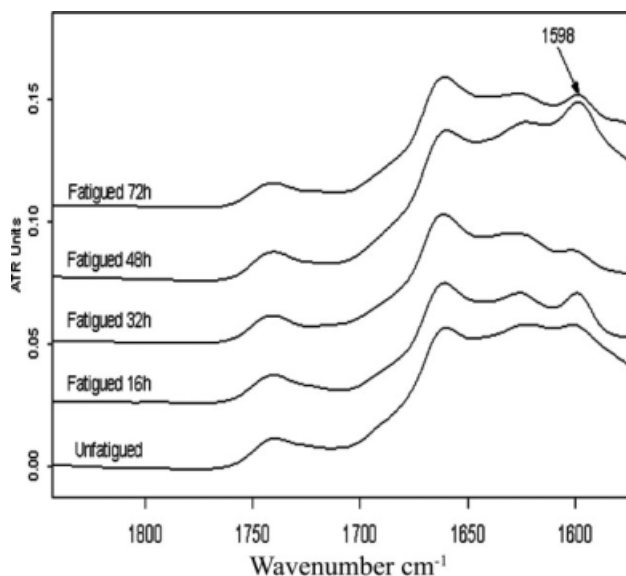


Figure 4 FTIR-ATR spectra of unfilled NR/4020 vulcanizates after various fatigue times.

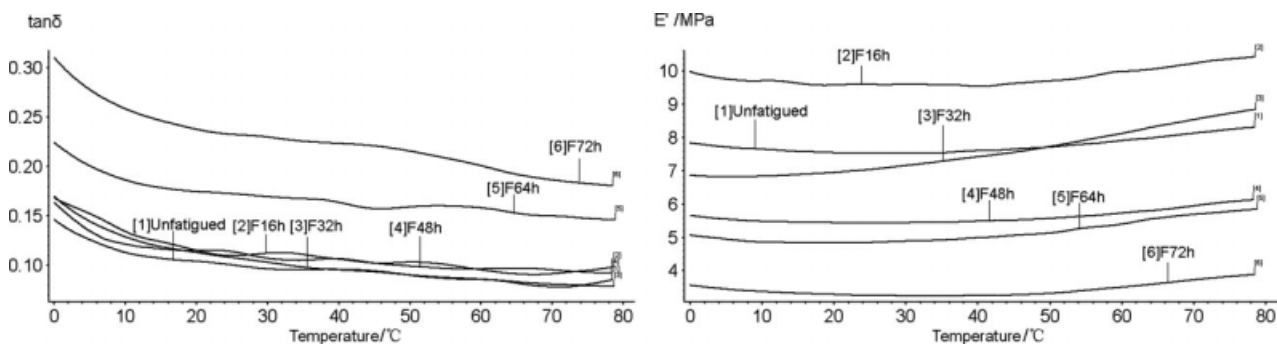


Figure 5 Dynamic mechanical properties of unfilled NR/4020 vulcanizates before and after tensile fatigue.

also induced some micropores to occur inside the sample. All those microscopic damages turned out to be the reasons that resulted in the deterioration of mechanical properties of samples, such as decrease of tensile strength and storage modulus and the increase of $\tan \delta$.

The antiaging function of 4020 in dynamically fatigued unfilled NR vulcanizates

Mechanical properties and crosslink density analysis

The change of mechanical properties and XLD as fatigue time is shown in Figure 3. It can be seen in Figure 3(a) that the tensile strength hardly decreases and the elongation at break slightly decreases as the

extension of fatigue time and the modulus at 100 and 300% [shown in Fig. 3(b)] increase little. Compared with the former research about the NR vulcanizates without 4020 where then mechanical properties deteriorated dramatically, it dedicated that 4020 showed a good antiaging function in fatigued NR vulcanizates.

It also can be seen in Figure 3 that XLD [see Fig. 3(c)] increases at the early fatigue stage and then turns stable; the mass percentage of cross-linked network A (M_c) slightly waves at the early fatigue stage and then starts to decrease after 32 h of fatigue. This might be attributed to the recrosslinking of free sulphur radicals $\cdot S_x \cdot$ resulted from scission of multisulphur bonds, which could cause an increase of crosslink

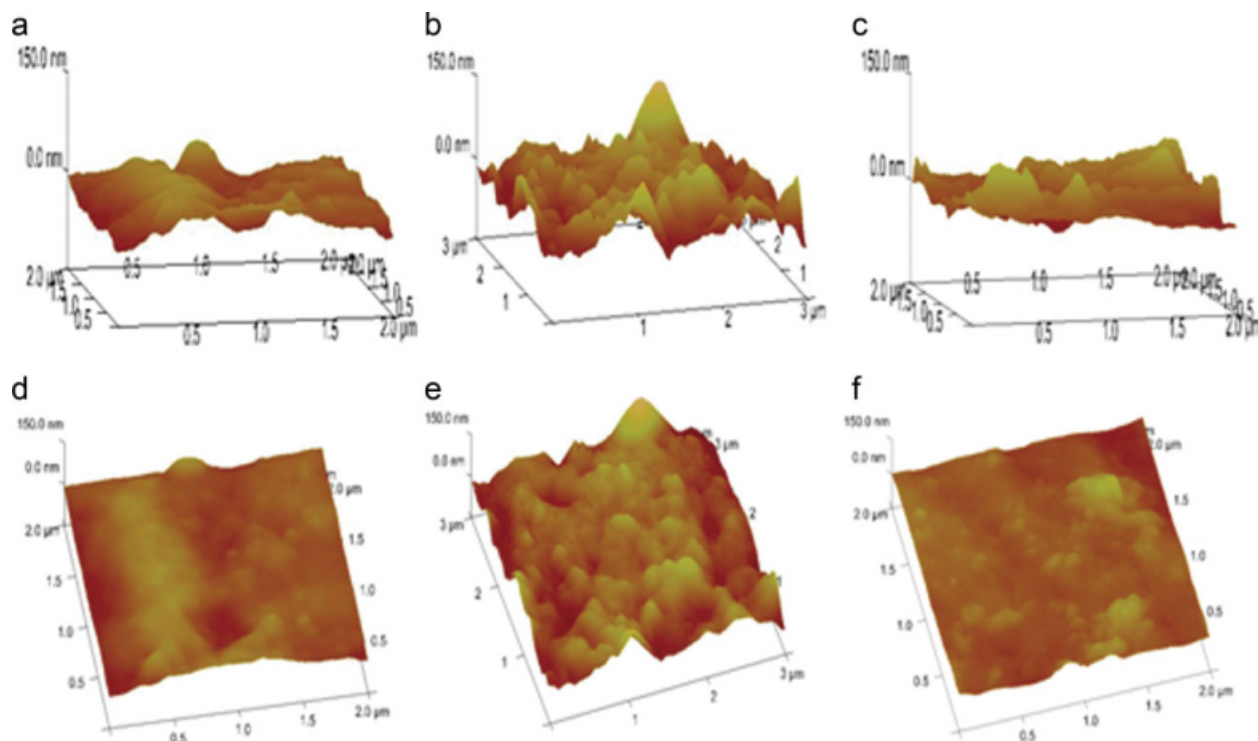


Figure 6 AFM photographs of NR and NR/4020 vulcanizates before and after tensile fatigue (a: F0h; b: F6h; c: with 4020 F32h; d: F0h; e: F6h; f: with 4020 F32h). [Color figure can be viewed in the online issue, which is available at www.interscience.wiley.com.]

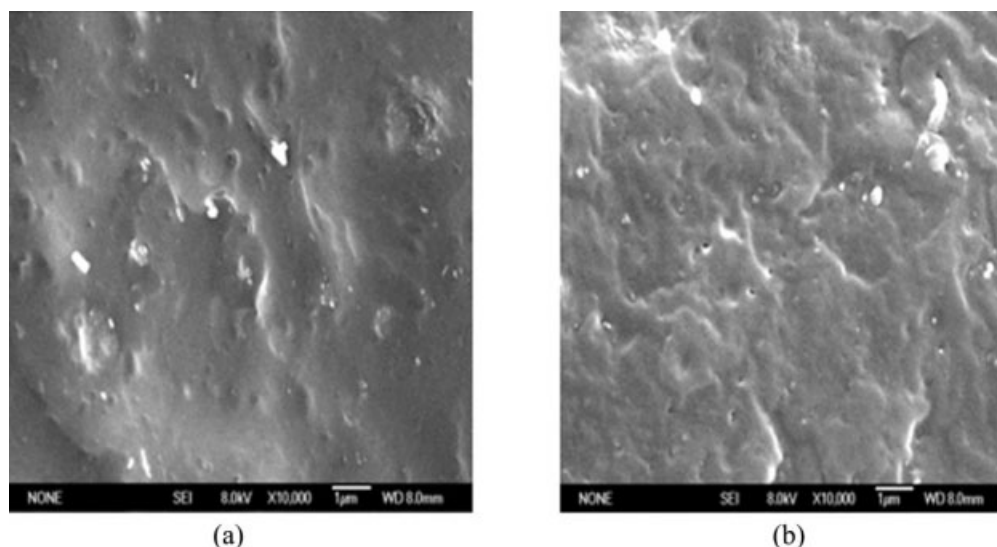


Figure 7 SEM photographs of NR and NR/4020 vulcanizate before and after tensile fatigue (a: F6h \times 10,000; b: with 4020 F32h \times 10,000).

density at the early fatigue stage, while at the latter fatigue stage, the scission of chains due to the constant stress buildup caused the decrease of A (Mc).

FTIR-ATR analysis

As seen in Figure 4, the absorption peak at 1598 cm^{-1} increases in different degrees after tensile fatigue, but it is weaker than that in vulcanizates without 4020.¹ The peak at 1598 cm^{-1} in tensile fatigue aged spectra can be assigned to the stretching vibration absorption of the double bond of conjugated dienes. According to the literature, during the decomposition of NR, the C—C bond between two α -methylenes can be broken, leading to free radicals and isomerization.^{2,3} The conjugated diene end groups might form from an isomerization of a broken backbone during tensile fatigue and structures such as conjugated dienes or trienes could also arise from a C—S bond scission if a hydrogen atom is abstracted from α - α -methylene.³ When 4020 was added, the free radicals from the C—C and C—S bond scission may be caught by 4020 to form a stable structure. Thus, the amount of conjugated dienes or trienes is reduced and the peaks at 1598 cm^{-1} did not change as much as those without 4020.

DMA analysis

The curves of $\tan \delta$ vs. temperature of $0\text{--}80^\circ\text{C}$ after various durations of tensile fatigue are shown in Figure 5(a). It can be seen that the $\tan \delta$ does not change much at the early fatigue stage, whereas it increases greatly at the latter fatigue stage. As for the vulcanizates without 4020, $\tan \delta$ changed significantly in all durations of tensile fatigue.

As can be seen in Figure 5(b), the storage modulus increases at 16 h of tensile fatigue, while it decreases after 32 h of tensile fatigue. The reason might be that at the early fatigue stage, 4020 had a strong antiaging function because of its much content; consequently the dynamic properties did not change obviously. In the latter stage, 4020 was almost consumed and lost its antiaging function, so the dynamic properties changed dramatically.

Morphology analysis

AFM photographs of NR and NR/4020 vulcanizates before and after tensile are shown in Figure 6. It can be seen that the surface roughness of NR vulcanizates with 4020 after 32 h of tensile fatigue had been improved greatly [Fig. 6(c)], compared with that of NR vulcanizates without 4020 [Fig. 6(b)]. This roughness difference can also be observed on the vertical pictures [Fig. 6(e,f)].

SEM photographs of NR and NR/4020 vulcanizates before and after tensile are shown in Figure 7. It can be seen that there are fewer and smaller micropores in NR vulcanizates with 4020 after 32 h of tensile fatigue than in NR vulcanizates without 4020 after 6 h fatigue.

Through the above morphology analysis, a conclusion is drawn that 4020 can reduce the expanding defect and forming during tensile fatiguing and has antiaging function in the NR vulcanizates.

CONCLUSIONS

1. AEM photographs showed that the surface roughness of unfilled NR vulcanizates became worse after tensile fatigue and the largest

undulation was as twice as that of unfatigued sample. SEM photographs showed that many micropore of 10^1 – 10^2 nm appeared after tensile fatigue.

2. The surface roughness of NR vulcanizates with 4020 after tensile fatigue became weaker than that of without 4020 and the micropores on cross section of samples were fewer and smaller.
3. The tensile properties and crosslink density of NR vulcanizates with 4020 after tensile fatigue did not change much and the absorption peak at 1598 cm^{-1} after tensile fatigue did not increase as much as that in NR vulcanizates without 4020.
4. In the early fatigue stage, $\tan \delta$ did not change obviously and E' increased slightly, while in the latter fatigue stage, $\tan \delta$ increased greatly and E' declined. The antiaging function of 4020 only presented at the early fatigue stage.

References

1. Zhang, P.; Shi, X. Y.; Li, J. G.; Zhao, S. G. *J Appl Polym Sci* 2008, 107, 1911.
2. Bramobauimo, H. K. *Polymer Compound Mechanical Chemistry*; Chemical Industry: Beijing, 1982; p 14.
3. Yang, Q. Z. *Modern Rubber Techniques*; China Petroleum: Beijing, 1995; p 333.